

Waveguide-Enhanced 2D-IR Spectroscopy for the Gas-Phase

Contact greg.greetham@stfc.ac.uk

G. M. Greetham, I. P. Clark and M. Towrie

Central Laser Facility, Science and Technology Facilities Council
Research Complex at Harwell, Rutherford Appleton Laboratory, Oxfordshire, OX11 0QX

D. Weidmann

Science & Technology Department, Science and Technology Facilities Council
Rutherford Appleton Laboratory, Oxfordshire, OX11 0QX

M. N. R. Ashfold and A. J. Orr-Ewing

School of Chemistry, University of Bristol
Cantock's Close, Bristol, BS8 1TS

Introduction

Ultrafast 2D-IR spectroscopy is a mature technique in application to the condensed phase, detailing many important structural dynamics and energy transfer processes in solution¹⁻⁴. Experiments involve ultrafast IR excitation of a sample, followed by time-resolved IR probing. The technique follows ultrafast changes in structure and/or vibrational energy transfer by monitoring the ways in which the IR (vibrational) spectrum of a sample varies with time and/or pump wavelength.

When studying the dynamics of any chemical reaction, the role of the environment cannot be ignored. For example, in many 2D-IR experiments, one must consider if observed changes in the vibrational spectrum are truly intra-molecular or solvent-mediated. Often, solution phase experiments will be performed under a variety of conditions (e.g. in different solvents^{5,6}) to help resolve such ambiguity. The possibility to perform experiments in the gas phase is an opportunity to remove solvent effects altogether.

Compared to the condensed-phase, gas-phase spectroscopy suffers from low sample concentrations and thus weak signal intensities. Normally, it is straightforward to increase the path length through the sample to regain signal intensity. However, transient pump – probe spectroscopy techniques, such as 2D-IR, require focusing of the beams onto the sample to generate significant population of excited state species to probe. This requirement to use focused beams (typically 100 μm diameter) limits the path length of a measurement to a few millimeters in the IR.

To increase the effective path length of a gas-phase 2D-IR measurement to 100 mm, we have performed experiments inside a square hollow IR waveguide⁷. Signal intensity is enhanced by more than an order of magnitude as compared with unguided measurements, despite some laser intensity losses incurred by transport through the waveguide.

Results

As a demonstration, we performed time-resolved 2D-IR measurements on the fluxional motion of iron pentacarbonyl ($\text{Fe}(\text{CO})_5$, fig. 1). 2D-IR spectra were taken of $\text{Fe}(\text{CO})_5$ vapor in free space and in a range of waveguide widths, showing increasing signal intensity with decreasing waveguide width. Figures 2A and B show the effect of the improved signal to noise that is achieved by guiding the IR beams, while figure 2C shows the magnitude of the signal enhancement achieved through decreasing the waveguide width. The 2D-IR spectra of this and other metal carbonyl samples have been well studied in solution-phase for comparison^{8,9}. However, the present measurements reveal new insights into the dynamics of $\text{Fe}(\text{CO})_5$ fluxional motion (fig. 1) in the gas phase.

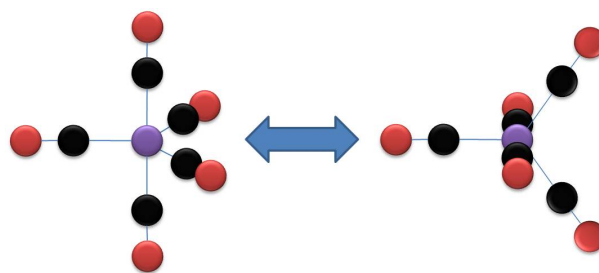


Figure 1. Fluxional motion of the $\text{Fe}(\text{CO})_5$ molecule.

It is important to note that these experiments were done at room temperature and atmospheric pressure. The enhancement in signal due to the waveguide enabled these high quality measurements to be made without having to increase the sample concentration by increased pressure or condensed phase sample heating to increase the vapor pressure.

Conclusions

A hollow waveguide has been applied to 2D-IR spectroscopy of gas-phase sample. The waveguide effectively increases the interaction path of the IR pump and probe beams with the low concentration gas-phase sample. We have demonstrated more than an order of magnitude signal enhancement over free gas measurements.

In comparison with solution-phase, dramatic changes in the timescale of the Berry pseudo-rotation of $\text{Fe}(\text{CO})_5$ have been observed in the gas-phase¹⁰.

Acknowledgements

The authors are grateful for access to the ULTRA laser facility. The STFC Centre for Instrumentation in Advanced Optics is acknowledged for the waveguide developments. MNRA and AJOE are grateful to EPSRC for funding via Programme Grant EP/G00224X, and AJOE thanks the ERC for support through Advanced Grant 290966 CAPRI.

References

1. P. Hamm, M. H. Lim and R. M. Hochstrasser, *J. Phys. Chem. B*, **102**, 6123, (1998).
2. M. C. Asplund, M. T. Zanni and R. M. Hochstrasser, *PNAS*, **97**, 8219, (2000).
3. C. J. Fecko, J. D. Eaves, J. J. Loparo, A. Tokmakoff and P. L. Geissler, *Science*, **301**, 1698, (2003).
4. N. T. Hunt, *Chem. Soc. Revs*, **38**, 1837, (2009).

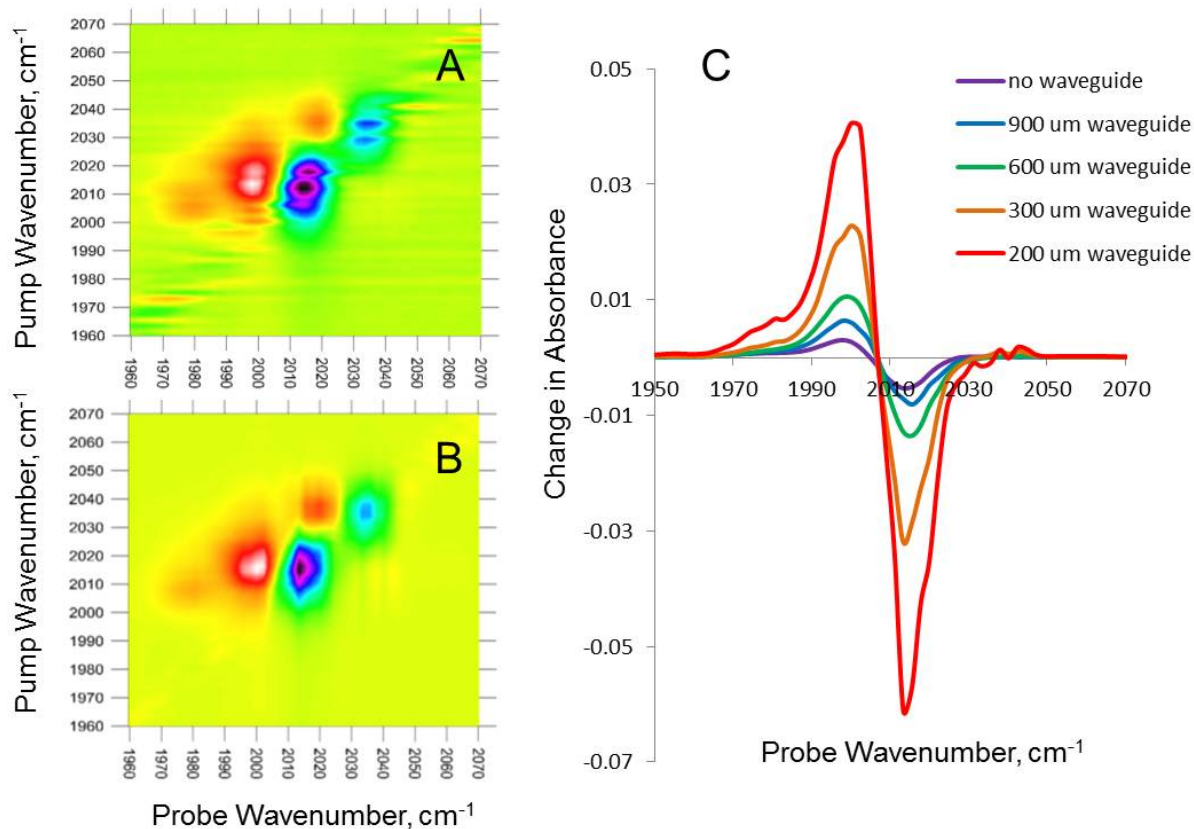


Figure 2. *A* and *B*, 2D-IR spectra of $\text{Fe}(\text{CO})_5$ vapor without and with the waveguide, respectively. *C* Pump – probe difference spectra of $\text{Fe}(\text{CO})_5$ vapor, pumping at 2013 cm^{-1} , in various waveguide conditions.

5. V. Botan, E. H. G. Backus, R. Pfister, A. Moretto, M. Crisma, C. Toniolo, P. H. Nguyen, G. Stock and P. Hamm, *PNAS*, **104**, 12749, (2007).
6. V. M. Kasyanenko, P. Keiffer and I. V. Rubtsov, *J. Chem. Phys.*, **136**, 144503, (2012).
7. D. Weidmann, B. J. Perrett, N. A. Macleod and R. M. Jenkins, *Optics Express*, **19**, 9074, (2011).
8. J. F. Cahoon, K. R. Sawyer, J. P. Schlegel and C. B. Harris, *Science*, **319**, 1820, (2008).
9. C. R. Baiz, P. L. McRobbie, J. M. Anna, E. Geva and K. J. Kubarych, *Accounts of Chemical Research*, **42**, 1395, (2009).
10. Results submitted for publication.

Ultrasensitive Dark-Field Microspectroscopy with a Super Continuum Source

Contact philipp.kukura@chem.ox.ac.uk

A Weigel, A Sebesta, P Kukura

Physical and Theoretical Chemistry

University of Oxford

South Parks Road

Oxford OX1 3QZ

Introduction

The advent of single particle optics has had a profound impact on a large variety of fields ranging from genetics all the way to quantum optics.¹ For truly nanoscopic particles and single emitters all current detection techniques rely exclusively on the efficient detection of fluorescence. Therefore, fundamental questions, such as the fate a quantum dot or a fluorophore, when it ceases to emit light (blinking or bleaching), still remain unsolved. Extinction of light, on the other hand, is largely independent of excited state relaxation and can detect particles even in their 'dark' state. The long-held notion that detection of the absorption of a single molecule is impossible was recently disproved.²⁻⁴ Extending such experiments from mere detection to broadband spectroscopy will provide a completely new view on single particle properties beyond the limitations of fluorescence spectroscopy.

Dark-field scattering microscopy directly detects the photons, which are elastically scattered by a particle away from the excitation beam. As fluorescence, the technique is in principle background-free, and therefore provides the ideal starting point for the development of an ultra-sensitive extinction spectrometer. Here, we have developed a detection geometry for dark field microspectroscopy that allows us to collect white light scattered from a particle with 95% of the numerical aperture of the objective. Losses in the detection arm are minimized with the use of a prism for dispersion. We present preliminary experiments on gold particles with 40 nm diameter are presented and show that the background suppression is large enough to measure the fluorescence of a single quantum dot in a scattering environment without the use of any filters.

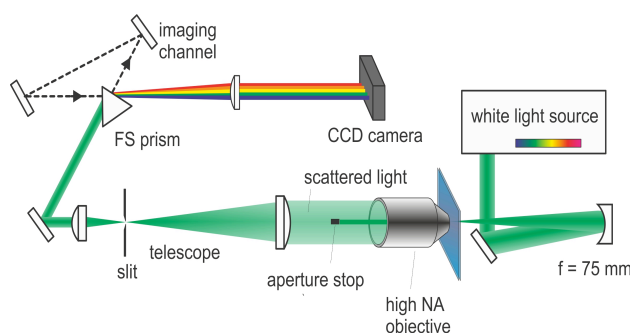


Figure 1: Setup of the dark-field microspectroscopy

Experimental approach

The achievable brightness of the collected scattering signal and the spatial resolution depend critically on the numerical aperture with which scattered photons can be detected. In conventional dark-field microscopy, background photons are avoided by blocking the transmitted or reflected illumination beam after the objective, at the expense of inherently reducing the effective numerical aperture. A classic example is annular illumination, which cropping of a relatively large part of the detection cone. Here, we illuminated the sample instead with a 75 mm focusing mirror under normal incidence from the front and block the narrow collimated beam after the objective with a small aperture stop. The 10 μm wide illumination spot is ideal for wide-field imaging of the sample. This allows us to measure the signals of a particle and its surroundings simultaneously.

The setup is illustrated in Fig. 1: The sample is illuminated with white light from a SuperK Extreme supercontinuum source (NKT Photonics), covering a spectral range from 430-800 nm. Transmitted and scattered light is collected with a 1.42 NA objective (Olympus PLAPON 60x). The aperture stop for blocking the illumination beam is only 1-2 mm in diameter, so that up to 95 % of the numerical aperture of the objective are used. The magnification is adjusted with a 3:1 telescope to optimize the imaging system for the relatively large pixel size of the CCD camera. A slit in the focal plane selects a single vertical slice of the 2-dimensional image, which is then dispersed with a fused silica prism and detected with a CCD camera (Rolera Thunder, QIMAGING). The use of a prism as the dispersing element reduces the losses to a minimum. The prism can be moved out of the beam path with a motorized translation stage (Agilis, Newport), opening an alternative imaging path (dashed black in Fig. 1). In this way the particle can be selected and precisely positioned with respect to the slit, ensuring reproducible detection with sub-nanometer spectral accuracy. Scattering cross section spectra were corrected by comparison with reference measurements of non-resonant scattering from latex beads.

Sample Preparation

Streptavidin-functionalized gold particles (BBI solutions) and Latex bead samples (Sigma, 100 nm diameter) in aqueous solution were deposited onto the cover slip by spin coating. Streptavidin-functionalized quantum dots with an emission maximum at 655 nm (Invitrogen) were immobilized on a cover slip surface by binding to biotinylated bovine serum albumin bound non-specifically to the surface of the coverslip.

Results and Discussion

Colloidal gold particles have been used for centuries for the staining of glass panes. Their color originates from a surface plasmon resonance around 530 nm and, in contrast to organic chromophores, they do not saturate upon illumination nor are subject to photobleaching. Together with their large scattering cross sections and stability this makes them ideal probes for a number of challenging applications in imaging and high-speed particle tracking.^{5,6} We used single gold particles with an average diameter of 40 nm on a glass coverslip for a first experiment. Typical measured scattering spectra of individual particles are shown in Fig. 2, left. Although the size variation of the investigated particles is only around 8 %, large differences in the scattering cross-section were observed. Dark-field microscopy is highly sensitive to size variation, because the signal strength scales with the sixth power of the particle diameter, so even a 10% reduction in particle size decreases the amount of scattered power by half. We remark that the collected images and spectra represent the highest signal-to-noise ratio dark-field images ever obtained of nanoscopic particles

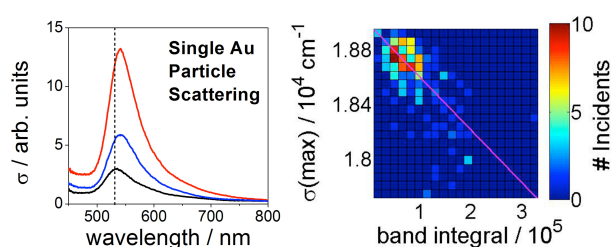


Figure 2: Scattering spectra of single gold particles with 40 nm average diameter (left) and histogram over the band maximum $\sigma(\max)$ and the band integral (right).

The spectra in Fig. 2 also exhibit a red shift of the resonance band with increasing particle scattering cross section. The 2D histogram in Fig. 2 summarizes the spectral scattering properties of 190 single gold particles. The orientation of the distribution along a diagonal demonstrates the correlation between scattering intensity and resonance band position. This result agrees with Mie theory, which predicts a red shift of the resonance for larger particles due to retardation effects and higher-order multipole contributions.⁷ Given the excellent images obtained for 40 nm particles, we believe that the detection limit will approach 10-20 nm particles, a several order of magnitude improvement in terms of scattered power of existing techniques.

The ultimate goal is to reach the sensitivity necessary to characterize luminescent particles in their dark state. One requirement is that fluorescence and scattering detection of a particle are synchronized, which is ideally achieved by measuring both on the same detector. For fluorescence measurements, the excitation light is commonly removed with a filter, but this is not necessary in spectrally resolved detection. As a model fluorophore we studied single quantum dots with an emission maximum around 655 nm, which were immobilized on a cover slip. As before, the sample was illuminated with white light, which was passed through a 600 nm short-pass filter. Fluorescence of the quantum dot can be seen as a bright line in the spectrally dispersed image in Fig. 3, top. Even without the use of filters, any background light is completely suppressed in the fluorescence region. At wavelengths below the excitation filter cut-off around 600 nm scattering signals are visible, mainly from non-fluorescent scatterers around the quantum dot. By forming the difference image between detection with the quantum dot in its 'on' and 'off' state, the pure quantum dot signal is isolated, see Fig. 3, bottom.

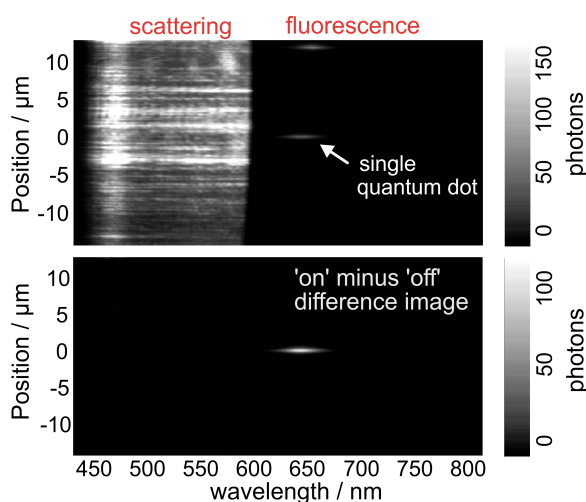


Figure 3: Dispersed Images of a single quantum dot in a scattering surrounding: Raw image (top) and 'on' minus 'off' difference image of the blinking quantum dot (bottom).

The semiconductor core of the measured quantum dots has a diameter of around 8 nm, and scattering of the quantum dot could not be identified at this stage. The strong size dependency of the scattering signal with the square of the volume renders the detection of small particles particularly demanding. However, when mixing the scattering field with a reference light field, the signal is only linearly dependent on the particle volume.⁸ Based on this technique the first direct detection of scattering from a single quantum dot was reported in 2009.⁹ It will be a future challenge to implement a similar approach into our spectrally resolved detection setup.

Summary and Conclusions

We have developed a novel dark-field microscope for visible scattering spectroscopy of nanoparticles with unprecedented sensitivity. Front illumination with a curved mirror allows us to use an aperture stop to block the transmitted excitation light, so that 95 % of the numerical aperture are used for detection. Subsequent losses are minimized by the use of a prism for dispersion. Scattering spectra of single gold nanoparticles with an average diameter of 40 nm were measured. The variation in the total scattering cross section was correlated with the position of the resonance band, and was assigned to a distribution in the particle size. The efficient suppression of background light was demonstrated by the simultaneous measurement of the fluorescence of a single quantum dot and scattering from its surrounding. Scattering from the quantum dot itself still evades detection, but can become feasible by implementing a heterodyne detection scheme, in future.

Acknowledgements

We are grateful to the Central Laser Facility for providing the SuperK Extreme supercontinuum source from their loan pool. A Weigel was supported by a Newton Fellowship of the Royal Society.

References

1. J. Hohlbein, K. Gryte, M. Heilemann, A.N. Kapanidis, *Phys. Biol.* **2010**, *7*, 031001.
2. P. Kukura, M. Celebrano, A. Renn, V. Sandoghar, *J. Phys. Chem. Lett.* **2010**, *1*, 3323.
3. S. Chong, W. Min, X. Sunney Xie, *J. Phys. Chem. Lett.* **2010**, *1*, 3316.
4. A. Gaiduk, M. Yorulmaz, P.V. Ruijgrok, M. Orrit, *Science* **2010**, *330*, 353.
5. S. Eustis, M. A. El-Sayed, *Chem. Soc. Rev.* **2006**, *35*, 209.
6. J. Ortega-Arroyo, P. Kukura, *Phys. Chem. Chem. Phys.* **2012**, *14*, 15625.
7. S. Link, M.A. El-Sayed, *J. Phys. Chem. B* **1999**, *103*, 8410.
8. K. Lindfors, T. Kalkbrenner, P. Stoller, V. Sandoghdar, *Phys. Rev. Lett.* **2004**, *93*, 037401.
9. P. Kukura, M. Celebrano, A. Renn, V. Sandoghdar, *Nano Lett.* **2009**, *9*, 926.